A 19-month Climatology of Marine Aerosol-Cloud-Radiation Properties derived from DOE ARM AMF deployment at the Azores: Part I: Cloud Fraction and Single-layered MBL cloud Properties

Xiquan Dong, Baike Xi, and Aaron Kennedy

Department of Atmospheric Sciences, University of North Dakota, Grand Forks, ND, USA

Patrick Minnis

Science Directorate, NASA Langley Research Center, Hampton, VA, USA

Robert Wood

Department of Atmospheric Sciences, University of Washington, Seattle, WA, USA

Submitted to the *Journal of Climate* (September 10, 2013)

Corresponding author address: Dr. Xiquan Dong, The Department of Atmospheric Sciences, University of North Dakota, 4149 Campus Road, Box 9006, Grand Forks, ND 58202-9006. Email: dong@aero.und.edu. Phone: 701-777-6991.

Abstract: A 19-month record of total, and single-layered low (0-3 km), middle (3-6 km), and high (> 6 km) cloud fractions (CFs), and the single-layered marine boundary layer (MBL) cloud macrophysical and microphysical properties has been generated from ground-based measurements taken at the ARM Azores site between June 2009 and December 2010. It documents the most comprehensive and longest dataset on marine cloud fraction and MBL cloud properties to date. The annual means of total CF, and single-layered low, middle, and high CFs derived from ARM radar-lidar observations are 0.702, 0.271, 0.01 and 0.106, respectively. More total and single-layered high CFs occurred during winter, while single-layered low CFs were greatest during summer. The diurnal cycles for both total and low CFs are stronger during summer than during winter. The CFs are bimodally distributed in the vertical with a lower peak at ~1 km and higher one between 8 and 11 km during all seasons, except summer, when only the low peak occurs. The persistent high pressure and dry conditions produce more single-layered MBL clouds and fewer total clouds during summer, while the low pressure and moist air masses during winter generate more total and multilayered clouds, and deep frontal clouds associated with midlatitude cyclones.

The seasonal variations of cloud heights and thickness are also associated with the seasonal synoptic patterns. The MBL cloud layer is low, warm and thin with large liquid water paths *LWP* and contents *LWC* during summer, whereas during winter it is higher, colder and thicker with reduced *LWP* and *LWC*. The cloud *LWP* and *LWC* values are greater at night than during daytime. The monthly mean daytime cloud droplet effective radius r_e values are nearly constant, while the droplet number concentration N_d basically follows the *LWC* variation. There is a strong correlation between cloud condensation nuclei *CCN* and N_d during January-May due to the frequent low-pressure systems because upward motion brings more surface *CCN* to cloud

base (well mixed boundary layer). During summer and autumn, the correlation between N_d and *CCN* is not as strong as that during January-May because downward motion from high pressure systems is predominate. Compared to the compiled aircraft in situ measurements during ASTEX, the cloud microphysical retrievals in this study agree very well with historical aircraft data. The different air mass sources over the ARM Azores site have significant impacts on the cloud microphysical properties and surface *CCN* as demonstrated by great variability in *CCN* and cloud microphysical properties during some months.

1. Introduction

Due to their substantial role in the earth's radiation budget, and consequently, their effect on the earth's climate, low-level stratiform clouds have been a topic of considerable interest since publication of the classic paper describing their physics (Lilly, 1968). Low-level stratiform clouds are often defined, from the satellite perspective, as clouds with tops beneath 680 hPa (~3.3 km), and include stratus, stratocumulus and shallow cumulus (Rossow and Schiffer, 1991). These low-level clouds can form within both deep and shallow marine boundary layers (MBL, defined as cloud-top heights lower than 3 km in this study). MBL clouds in the subtropical regions strongly influence the regional and global climate system (e.g., Klein and Hartmann 1993). The most extensive MBL clouds occur over the east side of subtropical oceans, and over the mid-latitude oceans under conditions of modest cold advection during periods of equatorward flow (Klein and Hartmann 1993). A strong temperature inversion at the top of the MBL, which is maintained by large-scale subsidence, combined with cold sea-surface temperatures, provides conditions favorable for MBL clouds (Lilly 1968). These MBL clouds are maintained by vertical mixing, primarily due to the strong longwave radiative cooling at cloud top because the radiative cooling generates turbulence to maintain an upward moisture flux (Albrecht et al. 1995; Paluch and Lenschow 1991; and Rémillard et al. 2012).

MBL clouds and their interactions with aerosols are extremely important components of the climate system (Wood 2012). Their treatment in climate models is one of the largest sources of uncertainty in predicting any potential future climate change (Wielicki et al. 1995; Houghton et al. 2001). Although many improvements have been made in the Coupled Model Intercomparison Project Phase 5 (CMIP5; Taylor et al. 2012; Klein et al. 2013; Jiang et al. 2012), MBL clouds are still a problem in climate models (e.g., Stanfield et al. 2013; Dolinar et al. 2013) and numerical weather prediction (NWP) models such as the NOAA/GFS (Yoo and Li 2012, Yoo et al. 2013). Because their structural and optical properties are strongly dependent upon interactions between aerosol/cloud microphysics and dynamics, these intricate interactions involve the formation of precipitation and its effect upon cloud dynamics, turbulence, and entrainment (Wood 2012). However, we still lack understanding of many key physical links between aerosol and cloud microphysical properties, nor do we have sufficient observations to accurately quantify the multivariate sensitivity of precipitation to cloud microphysical and macrophysical properties. Such studies are essential for the evaluation of both climate and process-based numerical models.

The climatic importance of the microphysical and macrophysical properties of MBL clouds, particularly the cloud fraction, cloud droplet effective radius (r_e) and number concentration (N_d), and liquid water content/path (*LWC/LWP*), is widely recognized. Early studies found that the albedo effect of these clouds is important and leads to a strong net cooling of the Earth system (Hartmann and Short 1980). Slingo (1990) used a climate model to show that a modest relative increase of 15-20% in the cloud fraction, coupled with a 15-20% decrease in r_e and a 20-30% increase in *LWP*, could balance the radiative perturbation associated with doubled CO_2 concentrations. Cess et al. (1990) compared 19 GCMs and found a variety of cloud feedback results, ranging from modestly negative to strongly positive, because various climate models have different representations of cloud microphysical and radiative properties. An updated comparison by Cess et al. (1996) showed a narrowed difference with most models producing modest cloud feedback, a result of corrections to cloud optical properties in the models, such as improved r_e values. The most recent studies, however, indicate little narrowing in the cloud feedback spread in the latest model versions (Soden and Vecchi 2011). It is therefore imperative to have more accurate MBL cloud microphysical properties through long-term ground-based observations, so that we can improve their representation in climate models.

The DOE Atmospheric Radiation Measurement (ARM) Mobile Facility (AMF) was deployed on Graciosa Island (the Azores, 39.09^{o}N, 28.03^{o}W) for approximately 19 months (June 2009-December 2010) to study the seasonal and diurnal variations of MBL clouds, and to increase our understanding of their formation-dissipation processes over the remote subtropical Northeast Atlantic Ocean (NEA) (Wood 2009). The long-term and comprehensive ground-based observations at the Graciosa Island site comprise an invaluable data source for investigating the seasonal and diurnal variations of MBL cloud fraction and macrophysical and microphysical properties, as well as their interactions with aerosols and large-scale synoptic patterns. The ARM AMF ground-based observations have ended the extended lapse in ground-based observations over the NEA since the 1992 Atlantic Stratocumulus Transition Experiment (ASTEX, Albrecht et al. 1995). The ASTEX field campaign provided a month-long record of ground-based observations and was one of the first successful deployments of millimeter radars to study MBL clouds.

As the first part of a series, this paper documents fundamental statistical information about seasonal and diurnal variations of (1) total and single-layered low (<3 km), middle and high (>6 km) cloud fractions, and their vertical distributions; and (2) single-layered MBL cloud (cloud-top heights < 3 km, including stratus, stratocumulus and shallow cumulus) macrophysical and microphysical properties over the Azores site during the period June 2009-December 2010. The present work, which uses 19 months of nearly continuous ground-based cloud observations, should provide the most comprehensive and reliable estimates, to date, of seasonal and diurnal variations of marine cloud fraction, MBL cloud macrophysical and microphysical properties, and the influence of large-scale dynamic patterns. The results should be valuable for advancing our understanding of the MBL cloud processes and properties and for enabling climate/forecast modelers to more fully evaluate their simulations over the NEA.

2. Datasets and large-scale synoptic patterns

The ARM AMF was deployed on the northern coast of Graciosa Island (39.09^{o}N, 28.03^{o}W) in the Azores in the Northeast Atlantic Ocean (NEA). As illustrated in Fig. 1, Graciosa Island is located in the northern part of the Azores where island effects on the measurements are minimal because winds are predominantly subtropical trades from the north and west as shown in Fig. 2. Graciosa Island is also an ideal location to study marine boundary layer (MBL) clouds because it is sufficiently remote to be clear of direct continental influence (1300 km from Europe). The Azores typically experiences relatively clean conditions advected from the central North Atlantic that produce nearly pristine MBL clouds, but periodically experiences episodes of polluted air advected from Western Europe, North Africa, and North America (Fig. 1) that enrich the MBL clouds with aerosols (Albrecht et al. 1995; Dong et al. 1997, Wood 2009). The NEA is a region of persistent but diverse subtropical MBL clouds. As illustrated in Fig. 2 , subsidence from a persistent high pressure system over the Azores during the summer months gave rise to relatively dry conditions (relative humidity RH ~ 65-75%) and a transition from an overcast stratocumulus regime to a broken trade cumulus regime. In contrast, low pressure systems tended to be located NNW of the Azores during the winter months, which induced anomalous westerly winds that transported moist air masses (RH~ 75-85%) from the North Atlantic to the Azores producing more multilayered clouds and deep frontal clouds associated with midlatitude cyclones.

The cloud macrophysical properties (such as fraction, height, thickness and temperature) used in this study are taken directly from the AMF merged soundings and radar, ceilometer, and lidar measurements. The primary AMF cloud observations and retrievals, as well as their uncertainties and references used in this study are listed in Table 1. The centerpiece of the cloud instrument array is the 95-GHz W-band ARM Cloud Radar (WACR) (Mead and Widener 2005). The WACR operates at a wavelength of 3.15 mm in a vertically pointing mode (a beamwidth of 0.19^o) and provides continuous profiles (2s temporal and 43-m vertical resolutions) of radar reflectivity from hydrometeors moving through the radar field of view, allowing the identification of clear and cloudy conditions. The WARC is sensitive enough (-50 dBZ at 2 km) to detect MBL small cloud droplets and large light-moderate drizzle drops (Rémillard et al. 2012).

The cloud fraction (CF) is simply the percentage of radar-lidar returns that are cloudy within a specified sampling time period (e.g., month), i.e., the ratio of the number of hours when both the radar and lidar/ceilometer detected clouds to the total number of hours when all measurements (radar/lidar/ceilometer) were available. This study uses ~12,950 hours for all-sky samples, which is 94% of all possible data during the 19-month period (for more details about the instruments up/down time, see Fig. 1 of Rémillard et al. 2012). The total cloud fraction CF_T is the fraction of time when a cloud is detected anywhere in the vertical column, the single-layered low cloud fraction CF_L is the fraction of time when low clouds (Z_{top} < 3 km) occur without clouds above them, the high cloud amount CF_H is determined for clouds having Z_{base} higher than 6 km with no clouds underneath, while middle clouds (CF_M) range from 3 to 6 km without any clouds below and above. Although CF_T, CF_L, CF_M, and CF_H are computed using the same denominator (all-sky samples), CF_T does not equal the sum of CF_L, CF_M, and CF_H

because CF_T includes all cloudy conditions, such as some deep convective clouds and multilayered clouds that did not satisfy our definitions of single-layered low/middle/high cloud layers. These cloud fractions should not be confused with the instantaneous hemispheric cloud fractions observed by satellite observations and surface observers (Dong et al. 2005).

Cloud-top height (Z_{top}) is derived from cloud radar reflectivity profiles and cloud-base height (Z_{base}) is derived from a composite of Belfort laser ceilometer, Micropluse Lidar (MPL), and cloud radar data (Clothiaux et al. 2000). Cloud-base and -top temperatures, T_{base} and T_{top}, respectively, are estimated from the ARM merged soundings (a linear temporal interpolation of ARM AMF rawinsonde soundings, ~4 times per day) using Z_{base} and Z_{top}. Cloud physical thickness (ΔZ) is simply the difference between Z_{top} and Z_{base}. The *LWP* is derived from the microwave radiometer brightness temperatures measured at 23.8 and 31.4 GHz using a statistical retrieval method (Liljegren et al. 2001). The AMF up- and down-looking standard Eppley Precision Spectral Pyranometers (PSPs) provide measurements of downwelling and upwelling broadband shortwave (SW, 0.3 to 3 μm) fluxes with uncertainties of ~10 Wm^{-2} (Long and Shi 2008).

The daytime microphysical and radiative properties of single-layered MBL clouds are retrieved from the SW and LWP data. A δ2-stream radiative transfer model is used to compute the downwelling SW flux. The retrieval scheme of Dong et al. (1997) is based on an iterative approach that varies cloud-droplet effective radius (r_e) and number concentration (N_d) in the radiative transfer calculations until the model-calculated solar transmission matches the measured one. Dong et al. (1998) parameterized the retrieved r_e as a function of *LWP*, the solar transmission and cosine of the solar zenith angle (μ_0). The optical depths are derived from the ratio of *LWP* and r_e. The retrieved and parameterized low-cloud microphysical properties have been validated by in-situ aircraft measurements at the midlatitude continental sites (Dong et al. 1998 and 2002; Dong and Mace 2003). Cloud condensation nuclei (*CCN*) were observed at 0.2% supersaturation by the ARM AMF Aerosol Observation System at the Azores (Jefferson 2010).

To help ensure reliable cloud microphysical retrievals, the cloudy cases selected in this study are single-layered and overcast low clouds that persist for approximately 2 hours over the AMF site. The MBL clouds include mostly stratus and stratocumulus, and some shallow cumulus clouds with cloud-top heights less than 3 km. Five criteria were established for choosing the conditions under which daytime cloud properties can be estimated. These criteria are (i) only single-layer and overcast low clouds are present as determined from cloud radar-lidar observations, (ii) Z_{top} < 3 km, (iii) *LWP* is between 20 and 700 g m^{-2}, (iv) μ_0 > 0.1, and (iv) the solar transmission (γ) is between 0.08 and 0.7. The physical reasons for using these five criteria are discussed in Dong et al. (2000). Approximately 1091 hours (~13,092 samples at 5-min resolution) of daytime data satisfied the above criteria during the 19-month period.

3. Cloud Fraction

In this section, the seasonal and diurnal variations of total and single-layered CFs, as well as their vertical distributions are presented in Figs. 3-5. The 10 CF categories at the ARM Azores site during the 19-month period are summarized in Table 2. Finally we discuss the similarities and differences between this study and Rémillard et al. (2012). Four seasons are defined as winter (December–February), spring (March–May), summer (June–August), and autumn (September–November) in this study.

a. Seasonal variation

The monthly variations of total cloud fraction (CF_T), and single-layered low (CF_L), middle (CF_M), and high (CF_H) cloud fractions during the 19-month period are illustrated in Fig. 3 and summarized in Table 2. The monthly means of CF_T decrease from winter to summer, reach a minimum during September, and then gradually increase from September to December with an annual average of 0.702. The CF_L values remain nearly constant (0.22) from Janunary to May followed by a significant increase to 0.38 during June-August, and then fluctuate from 0.17 to 0.34 during September-December. Notice that during summer, the majority of clouds are single-layered low clouds (CF_L=0.38 vs. CF_T=0.61) due to a persistent high pressure system (Fig. 2) and nearly 100% inversion-topped MBLs (Fig. 5a in Rémillard et al. 2012). Multilayered clouds are the majority during winter when the sum of all single-layered clouds is only ~0.37 (vs. CF_T=0.8). The monthly variation of CF_H is almost the same as that of CF_T, decreasing from winter to summer, but mirrors the variation of CF_L. Single-layered middle clouds occur least frequently and are seasonally invariant. The annual means of CF_L, CF_M and CF_H are 0.271, 0.01 and 0.106, respectively, indicating that both single-layered middle and high clouds occur much less frequently than single-layered low clouds at the Azores in this study.

b. Diurnal cycle

Figure 4 shows the hourly means of CF_T and CF_L for all of the data and for winter and summer separately. The hourly mean *CFs* were calculated from all samples in that local hour (such as between 1-2 am, presented at 2 am in Fig. 4) during the 19-month period. For the annual and winter periods, the hourly means of their CF_T and CF_L are relatively invariant. During summer, however, there are strong diurnal variations in both CF_T and CF_L where the CF_T variation basically follows the CF_L variation (Fig. 4c). For example, both *CFs* remain nearly constant from midnight [00 local time (LT)] to 10 LT, decrease from 11 to 15 LT followed by an increase to 19 LT, and finally level off for the remainder of the night. The annual, winter, and summer hourly mean CF_T differences (ΔCF_T=*Max.*–*Min.*) are 0.041 (0.041/0.70=5.9%), 0.103 (12.9%), and 0.173 (27.6%), respectively. For the CF_L differences, they are 0.065 (22.6%), 0.086 (40%), and 0.208 (56.2%), respectively. The CF_L and CF_T maxima occur during the night and morning with minima during afternoon. This day-night difference is most pronounced during summer, which is consistent with the results in Wood (2012, Fig. 8a) although his definition of low cloud amount differs from that in this study. This strong diurnal variation in CF_L results from mixing driven by nocturnal longwave radiative cooling at cloud top that is not countered by solar absorption at night (Albrecht et al. 1995; Paluch and Lenschow 1991; Wood 2012; Rémillard et al. 2012). During the day, the absorption of solar radiation near cloud top warms the cloud layer and partially offsets the longwave radiative cooling, which suppresses the turbulence and cloud formation within the MBL.

c. Vertical distribution

Figure 5 shows the annual and seasonal mean vertical distributions of *CF* derived from the ARM radar-lidar observations with a 43-m vertical resolution during the 19-month period. During summer, the *CF* profile is strongly peaked at 1 km with typical *CF* values of ~0.05 above 2 km. A very minor secondary maximum is seen near 11 km. For the other seasons, and hence, for the annual mean, the *CF* vertical distributions are strongly bimodal, with the primary and secondary peaks at ~1 km and between 8 and 9 km, respectively. The winter and spring seasons experience not only more middle and high clouds, but also more low clouds than other seasons, despite the summertime maximum in single-layer low clouds. The cold season low-cloud maximum is due to the increased multilayered clouds. The seasonal synoptic patterns (Fig. 2) provide strong support for the results in Figs. 3-5. That is, the persistent high pressure and dry conditions explain more single-layered MBL clouds and fewer total clouds during the summer months, while the low pressure and moist air masses during the winter months result in more occurrences of total and multilayered clouds, and more deep frontal clouds associated with midlatitude cyclones.

To further investigate the *CF* vertical distributions, the ARM radar-lidar-derived *CFs* have been classified into 10 categories (see summary in Table 2) that should represent different cloud formation and dissipation processes and different large-scale dynamics. The definitions of these 10 categories have been discussed in detail by Xi et al. (2010). Basically, the definitions of single-layered low/middle/high clouds are the same as in Fig. 3. The percentages of categories 1-3 in Table 2 are the same as the results in Fig. 3, while the percentages in both categories 4 and 6 represent cumulus or convective clouds and the percentage in category 5 is for physically thick cirrus clouds. Technically speaking, categories 4-6 belong to single-layered clouds, but they do not fit in the definitions of single-layered low, middle and high clouds in this study, while categories 7-10 are multilayered clouds. Based on this discussion, the single-layered (sum of categories 1-6) and multilayered (sum of categories 7-10) CFs are 0.468 and 0.233 for the annual mean, 0.496 and 0.305 for winter, and 0.485 and 0.127 for summer. The results in Table 2 reveal the magnitude of the winter-summer difference in multilayered cloud CFs. Table 2 also shows that there are more deep frontal clouds associated with midlatitude cyclones and/or convective clouds during winter than during summer at the Azores (category 6=0.064 and 0.007 for winter and summer, respectively).

d. Discussion

Rémillard et al. (2012) provided the operational status of ARM AMF WACR, ceilometer, and MWR, as well as different types of cloud occurrences during the 19-month period at the Azores. They primarily focused on MBL clouds and investigated their cloud structural and dynamical properties, such as cumulus and stratocumulus cloud fractions and associated *LWP*, drizzle and precipitation. In this study, we provide the statistical results of total and single-layered low, middle and high cloud fractions, as well as their vertical distributions, but do not provide different MBL cloud types and drizzle/precipitation. There are some similarities and differences between these two studies. For example, their low clouds were defined as cloud-top heights lower than 3 km, same as this study, but their middle and high clouds were defined as cloud-base heights above 3 and 7 km, respectively (Table 2 in Rémillard et al. 2012). Also their low, middle and high cloud occurrences (Fig. 2b in Rémillard et al. 2012) represented all cloudy conditions (single- and multi-layer), while the monthly mean CFs in Fig. 3 are representative of single-layered low, middle and high clouds. Nevertheless, their total cloud occurrence (Fig. 2a in Rémillard et al. 2012) was the same as the CF_T in Fig. 3, confirming that both studies used the same datasets and had the same total cloud fraction during the 19-month period. Although there are some overlaps between these two studies, they complement each other. Therefore the combination of these two studies will provide a more complete characterization of the marine clouds and MBL clouds at the Azores.

4. Single-layered low cloud properties

In this section, all cloud properties are derived from the single-layered low clouds, those with cloud-top heights below 3 km without any overlying clouds. These low-level clouds are defined as MBL clouds here although these clouds can form within both deep and shallow MBLs and differ slightly from the traditional definition of MBL clouds. In particular, the monthly mean daytime MBL cloud macrophysical properties, such as cloud-base and –top heights and temperatures and thickness, are presented in Fig. 6, and daytime microphysical properties are presented in Fig. 8. Their corresponding daytime (and night) frequency distribution functions (PDF) and cumulative distribution functions (CDF) are illustrated in Figs. 7 and 9, respectively. Their seasonal and yearly mean, standard deviation, median, and mode values are listed in Table 3. The diurnal variations of MBL cloud macrophysical and microphysical properties are shown in Fig. 10.

a. Macrophysical properties

Monthly mean daytime MBL cloud macrophysical properties derived from the 19-month Azores dataset along with variations about the means are represented as box-and-whiskers plots in Fig. 6. In each plot, bottom and top of each whisker represent the 5th and 95th percentiles of the probability distribution functions (PDF), bottom and top of each box represent 25th and 75th percentiles of the PDF, and the shorter and longer lines across each box represent the median and mean, respectively. The distribution at the far right (ANN) of each plot shows the cumulative statistics from the entire daytime dataset during the 19-month period. The average for the dataset is given by the horizontal line extending across the entire plot. Monthly mean cloud-base and –top heights (Figs. 6a and 6b) are above their annual means (Z_{base} = 1.016 km, Z_{top} = 1.575 km) from December through May followed by a significant drop in June, and then remain below or close to their annual means until November. Cloud thickness ($\Delta Z=Z_{top}$ - Z_{base}) in Fig. 6c basically follows the cloud layer variation. That is, the cloud depth, on average, is about 100 m thicker during winter and spring than during summer and autumn. These results are also consistent with those in Fig. 5 where the primary frequency maxima during winter and spring occur at slightly higher altitudes than those during summer and autumn. The annual mean cloud-base (T_{base}) and –top temperatures (T_{top}) are 281.8 and 280.1 K, respectively. The monthly T_{base} and T_{top} averages basically follow the seasonal variation of surface temperature and mirror their height variations, such as being below their annual means from December to May, and above them from June to November. These results indicate that the MBL cloud layer, depth and temperature are deeper, thicker and cooler, respectively, from December to May than those from June to November in this study. This result is consistent with estimates of the seasonal variation of low clouds off the Californian coast (Lin et al. 2009).

The seasonal variations of cloud height and thickness in Fig. 6 are also consistent with the seasonal synoptic patterns (Fig. 2). That is, the lower cloud-base and –top heights and smaller cloud thickness during summer are associated with the persistent high pressure and dry conditions. On the other hand, the dominant low pressure systems and moist air masses during the winter months result in more deep frontal clouds associated with midlatitude cyclones, which will make the MBL clouds deeper and thicker.

Figure 7 shows the probability distribution functions (PDF) and cumulative distribution functions (CDF) of cloud macrophysical properties for both day (solid line) and night (dashed line) from all 5-min samples at the ARM Azores site during the 19-month period. As demonstrated in Fig. 7 and summarized in Table 3, the daytime and nighttime PDFs and CDFs of the MBL cloud macrophysical properties are very similar. The mean, median and mode values of Z_{top} and Z_{top} are nearly same year around, indicating a near-normal distribution of MBL cloud-base and -top heights at the Azores. ΔZ has a positive skew, while T_{base} and T_{top} have a negative skew. The cloud bases are nearly all below 2 km and peak at 0.8-1 km. Most cloud tops are located between 1 and 2 km, although 20% of the Z_{top} values are below 1 km, and 20% are above 2 km. Because there are no significant differences in cloud-base and –top height between day and night, the cloud thicknesses during day and night are also nearly the same with mode values of 0.2-0.4 km. Nearly 80% of the clouds are less than 1 km thick. Almost all T_{base} and T_{top} values are warmer than 270 K, indicating the MBL clouds are liquid-phase clouds in this study. Both T_{base} and T_{top} peak at 285-290 K and have tails toward to a lower temperature (~ 270 K). The rise in lower T_{top} values at night coincides with the rise in Z_{top} to values > 1.6 km.

b. Microphysical properties

Monthly means of the daytime cloud microphysical properties, *LWP*, *LWC*, r_e, N_d, and optical depth (τ), as well as surface *CCN*, are shown in Fig. 8. Their corresponding daytime (and nighttime for *LWP* and *LWC*) PDFs and CDFs are plotted in Fig. 9 and their seasonal and yearly mean, standard deviation, median, and mode values are listed in Table 3. As demonstrated in Figs. 8a (8b), the monthly means of *LWP* (*LWC*) exceed the annual mean from April to July (for *LWC* from April to September), while averages for other months fall below the annual mean. These results are also reflected in their seasonal means listed in Table 3 where the *LWP* and *LWC* values during spring and summer are larger than those during winter and autumn. The nighttime *LWP* and *LWC* averages are about 30 gm^{-2} and 0.04 gm^{-3} larger, respectively, than their daytime values year around, consistent with satellite measurements (e.g., Wood et al. 2002, O'Dell et al. 2008). Both the median and mode values in *LWP* and *LWC* are lower than their means suggesting that there is a positive skew in *LWP* and *LWC* distributions. As illustrated in Figs. 9a and 9b, there are obviously more large *LWP* and *LWC* values during night than during day.

The monthly mean r_e values are nearly constant and fluctuate within 1 μm around the annual mean of 12.4 μm, except for January and November when the monthly r_e means are 1.8 μm and 1.1 μm, respectively, below the annual mean. These annual and monthly means represent the typical MBL cloud droplet effective radius (e.g., Dong et al. 1997, Miles et al. 2000). As listed in Table 3, the annual r_e mean, standard deviation, median, and mode are 12.5, 4.6, 11.9, and 11 μm, respectively. The PDF in Fig. 9 and nearly same mean, median, and mode r_e values indicate a near-normal distribution of r_e with a peak at 10-12 μm. Because τ was calculated from the ratio of *LWP* to r_e, its monthly means are nearly the same as the *LWP* variation given the nearly constant r_e year round. Its annual mean is 13.1 with peaks from 5 to 15.

The monthly mean N_d values fluctuate around the annual mean (82 cm^{-3}) with a long tail toward to higher values as shown in Figs. 8d and 9d. Nearly 80% of the N_d means are less than 100 cm^{-3}. The method ($\sim LWC/r_e^3$) to calculate N_d assumes a lognormal size distribution (σ_x=0.38, Miles et al. 2000). With nearly constant r_e value year around, the monthly variation of N_d basically follows the *LWC* variation (Figs. 8b-d) exception during January and November because the r_e values during those two months are much smaller than the annual mean. The monthly mean surface *CCN* values have a relatively large variation around the annual mean (215 cm^{-3}) with a minimum of 129 cm^{-3} during February and a maximum of 322 cm^{-3} in April. The winter (266 cm^{-3}) and spring means (235 cm^{-3}) are much higher than the summer (193) and autumn (196 cm^{-3}). The monthly variation of *CCN* follows the N_d variation during January-May due to the frequent low-pressure systems because upward motion can bring more surface *CCN* to cloud base (well mixed boundary layer). During summer and autumn, the correlation between N_d and *CCN* is not as strong as that during January-May because downward motion from high pressure systems is dominant. The PDF of *CCN* (at 0.2% supersaturation) is similar to that of N_d with peak values ranging from 50 to 250 cm^{-3}.

Combining the daytime macrophysical properties discussed in Section 4a and listed in Table 3, we can draw the following conclusion: during summer the MBL cloud layer is shallow, thin and warm with large *LWP* and *LWC*, whereas during winter it is deep, thick and cold with less *LWP* and *LWC*. Note that this conclusion is totally opposite to those at the ARM SGP site (Table 2 in Dong et al. 2005), that is, the low cloud layers at the SGP are deeper, thicker, and warmer with less *LWP* and *LWC* during summer than those during winter. These different cloud properties may be impacted by different synoptic patterns and air masses, and/or physical processes/mechanisms. Therefore a further study to investigate these differences is warranted.

c. Diurnal variation

The hourly mean single-layered MBL cloud macrophysical and microphysical properties are calculated from all available samples in each hour from the 19-month ARM Azores dataset and are illustrated in Fig. 10. The hourly mean Z_{base}, Z_{top}, and ΔZ are almost constants without significant day-night differences. The hourly mean cloud-base and –top temperatures fluctuate around their daily means within 1 K (Figs. 10b) with the lowest temperature during sunrise or early morning (~6-8 LT) and the highest temperature during late afternoon (18 LT). These results indicate that there are no strong diurnal variations in the MBL cloud macrophysical properties at the Azores.

Strong diurnal variations, however, are seen in the cloud microphysical properties, *LWP* and *LWC* (Figs. 10c-d). There are larger *LWP* values at night (140 gm^{-2}) than those during daytime (109 gm^{-2}) with a semi-diurnal cycle peaked at 05 LT and 21 LT, respectively. Because the diurnal variation in cloud thickness is small, the hourly mean *LWCs* are primarily determined by the *LWP* values (Fig. 10d). Although the day-night *LWC* difference is small (LWC_{max} - LWC_{min}=0.067 gm^{-3}), it is apparent that the *LWC* values during night are greater than those during daytime. This result suggests that solar absorption at cloud top not only suppresses the turbulence generated through nocturnal longwave radiative cooling at cloud top and MBL cloud formation, but also reduces *LWC* adiabaticity.

Based on the investigation of hourly means (Figs. 10a-d), we can draw the following conclusion. The cloud-base and –top heights and temperatures, and cloud depth, are nearly invariant. There are semi-diurnal cycles in both *LWP* and *LWC* with larger values during night than during daytime. The results in this study are very similar to those derived from ship-based meteorological data during the 2008 VAMOS Ocean-Cloud-Atmosphere-Land Study Regional Experiment (VOCALS-REx) over the southeast Pacific Ocean (Burleyson et al. 2013). Figures 10e-h show the daytime hourly mean r_e, N_d, *CCN* and optical depth based on available retrievals. Similar to its seasonal variation, the hourly variation of r_e is also small. The hourly variation of N_d ($\sim LWC/r_e^3$) basically follows the *LWC* variation with some modification by r_e. The hourly variation of *CCN* is also flat with low values at sunrise and high ones at late afternoon. For cloud optical depth, the diurnal variation is similar to its seasonal variation, largely following that of *LWP*.

d. Discussion

Table 4 summarizes the MBL cloud *LWC*, r_e, N_d and *CCN* means retrieved for this study, and measured in situ by aircraft during the ASTEX IOP during June 1992. Miles et al. (2000) generated a comprehensive database of MBL cloud microphysical properties derived from aircraft in situ measurements during various field experiments, including ASTEX, conducted before the year 2000. The MBL cloud properties, such as *LWC*, r_e, and N_d, change significantly from different field experiments over different climatic regimes with the means (standard deviations) of 0.18 gm^{-3} (0.14 gm^{-3}), 9.6 μm (2.4 μm) and 74 cm^{-3} (45 cm^{-3}). Yum and Hudson (2002) processed a total of 17 ASTEX aircraft flights, and classified them into 11 maritime and 6 continental air masses. The summarized maritime (continental) cloud microphysical properties of *LWC*, r_e, N_d and *CCN* (0.6% supersaturation) are 0.164 gm^{-3} (0.119 gm^{-3}), 8.2 μm (6.1 μm), 86 cm^{-3} (183 cm^{-3}), and 163 cm^{-3} (1023 cm^{-3}), respectively. These aircraft in situ measurements are consistent with the remotely-sensed MBL cloud microphysical properties documented in this study although the aircraft data were all collected during a single month (June 1992). The monthly means of daytime *LWC*, r_e, N_d and *CCN* during June are 0.25 gm^{-3}, 12.4 μm, 91 cm^{-3}and 169 cm^{-3} in this study, and agree very well with aircraft data.

Garrett and Hobbs (1995) examined two different cases: one with a clean marine air mass (12 June 1995) and a second adjacent, continentally-influenced air mass (22 June 1995) near the Azores using aircraft data. Hudson and Li (1995) examined the 17 June 1995 case near the Azores using aircraft data and found two distinguishable air masses. Dong et al. (1997) found the similar MBL cloud microphysical properties retrieved from the ground-based measurements for the 17 June case. All these results and the summarized maritime and continental cloud microphysical properties in Table 1 of Yum and Hudson (2002) indicate that the continentally polluted air masses can be transported to the Azores and impact MBL cloud microphysical properties. For example, the polluted air masses can result in higher *CCN*, N_d, and smaller r_e, while the clean air mass can lead to lower *CCN*, N_d, and larger r_e values although their *LWC* values are close to each other. The different air mass sources over the ARM Azores site will significantly impact our cloud microphysical property retrievals and surface *CCN* as demonstrated great variability in *CCN* and cloud microphysical properties in some months.

Notice that the correlation between *CCN* and N_d in our study is not as strong as reported in the aircraft studies discussed above because *CCN* was measured at the surface here, while N_d was retrieved in the MBL cloud layer. Without aircraft in situ measurements, it is difficult to quantitatively answer how much of the surface *CCN* can be converted to N_d, and whether or not the surface *CCN* can represent the cloud base *CCN* information. To validate these ground-based observations and retrievals directly, it is necessary to make a direct comparison between aircraft data and surface retrievals

5. Summary and conclusions

This first part of a series of papers describing the climatological MBL aerosol, cloud and radiative properties at the ARM Azores site documents the most comprehensive and longest ground-based dataset on marine cloud fraction and MBL cloud macrophysical and microphysical properties to date. A 19-month record of total, and single-layered low (0-3 km), middle (3-6 km), and high (> 6 km) cloud fractions, and the single-layered MBL cloud macrophysical and microphysical properties was generated from ground-based measurements taken at the ARM Azores site between June 2009 and December 2010. This comprehensive dataset was used to examine the seasonal and diurnal variations, vertical distributions, as well as the impact of large-scale synoptic patterns on these MBL cloud fractions and properties. We have also compared the results in this study with other studies using aircraft in situ measurements during the ASTEX. From the 19-month record of ground-based observations and retrievals, we have the following conclusions:

1) The monthly variations of total cloud fraction, and single-layered low, middle, and high cloud fractions show that CF_T and CF_H were greatest during winter, while CF_L peaked during

summer. Midlevel clouds occurred least frequently and were nearly invariant over the annual cycle. Both CF_T and CF_L undergo diurnal cycles that are more pronounced during summer than during other seasons. The *CF* occurring in a given altitude layer is bimodally distributed year around with a lower peak at ~1 km and a higher one between 8 and 11 km. During summer the high cloud peak is less significant than during other seasons. The persistent high pressure and dry conditions result in more single-layered MBL clouds and less total cloudiness during summer, while the frequent low-pressure systems and moist air masses during winter generate more total and multilayered clouds, and deep frontal clouds associated with midlatitude cyclones. Because this study and Rémillard et al. (2012) complement each other, together they provide a more complete characterization of marine clouds and MBL clouds at the Azores.

2) The seasonal variations of cloud heights and thickness are strongly associated with the seasonal synoptic patterns. For example, the lower cloud-base and –top heights, and diminished cloud thickness during summer are associated with the persistent high pressure and dry conditions. In contrast, the predominant low-pressure systems and moist air masses during winter result in more deep frontal clouds associated with midlatitude cyclones, which will make the MBL cloud layer deeper and thicker. Therefore, we can draw the following conclusion: during summer the MBL cloud layer is shallow, thin and warm with large *LWP* and *LWC*, whereas during winter it is deep, thick and cold with less *LWP* and *LWC*. Cloud-base and –top heights and temperatures, and cloud depth are nearly invariant over the diurnal. There are semi-diurnal cycles in both *LWP* and *LWC* with larger values during night than during daytime.

3) The monthly daytime r_e means are nearly constant and fluctuate within ±1 μm of the annual mean of 12.4 μm. The monthly variation of N_d basically follows the *LWC* variation. There is a strong correlation between *CCN* and N_d during January-May due to the frequent low-pressure systems. During summer and autumn, the correlation between N_d and *CCN* is weaker than during January-May because downward motion from high pressure systems is dominant. Although taken during different periods, the cloud microphysical retrievals in this study agree very well with aircraft data taken during ASTEX. The different air mass sources over the ARM Azores site significantly impacted the cloud microphysical property retrievals and surface *CCN* as demonstrated by the great variability in *CCN* and cloud microphysical properties during some months.

These results can serve as a baseline for studying the MBL cloud fractions, macrophysical and microphysical properties. These results can also serve as ground truth for validating satellite retrieved MBL cloud properties at the Azores (Xi et al. 2013). This 19-month dataset over the ARM Azores site should also provide statistically reliable estimates of the monthly and diurnal variations of cloud fractions and properties for climate and numerical modelers to verify their simulated MBL cloud fractions and properties. The conclusions reached here are based only the surface observations, and further validation study using coincident aircraft in situ measurements is required. Future installments of this series will report on the impact of clouds on surface and TOA radiation budgets, and MBL aerosol-cloud interactions at the Azores.

Acknowledgments:

The data were obtained from the Atmospheric Radiation Measurement (ARM) Program sponsored by the U.S. Department of Energy (DOE) Office of Energy Research, Office of Health and Environmental Research, Environmental Sciences Division. Figure 1 was generated by Mr. Timothy Logan at UND. This study was primarily supported by the NASA CERES project at University of North Dakota project under Grant NNX10AI05G. The University of North Dakota authors were also supported by DOE ASR project at University of North Dakota under Grant with award number DE-SC0008468. Dr. Robert Wood was supported by DOE ASR project at University of Washington with award number DE-SC0006865MOD0002.

References

Albrecht, B. A., C. S. Breherton, D. Johnson, W. H. Scubert, and A.S. Frisch, 1995: The Atlantic Stratocumulus Transition Experiment-ASTEX. *Bull. Amer. Meteor. Soc.*, **76**, 1-16.

Burleyson, C. D., S. P. de Szoeke, S. E. Yuter, M. Wilbanks, W.A. Brewer, 2013: Observations of the diurnal cycle of southeast Pacific marine stratocumulus clouds and precipitation. *J. Atmos. Sci.* (revised).

Cess, R. D., and Coauthors, 1990: Intercomparison and interpretation of climate feedback processes in 19 atmospheric general circulation models. *J. Geophys. Res.*, **95**, 16 601-16 615.

Cess, R. D., and Coauthors, 1996: Cloud feedback in atmospheric general circulation models: An update. *J. Geophys. Res.*, **101**, 12 791–12 794.

Clothiaux, E. E., T. P. Ackerman, G. G. Mace, K. P. Moran, R. T. Marchand, M. A. Miller, and B. E. Martner, 2000: Objective determination of cloud heights and radar reflectivities using a combination of active remote sensors at the Atmospheric Radiation Measurement Program Cloud and Radiation Test Bed (ARM CART) sites. *J. Appl. Meteor.*, **39**, 645-665.

Dong, X., T. P. Ackerman, E. E. Clothiaux, P. Pilewskie, and Y. Han, 1997: Microphysical and Radiative properties of stratiform clouds deduced from ground-based measurements. *J. Geophys. Res.*, **102**, 23,829-23,843.

Dong, X., T. P. Ackerman, and E. E. Clothiaux, 1998: Parameterizations of microphysical and Shortwave radiative properties of boundary layer stratus from ground-based measurements. *J. Geophys. Res*. **102**, 31,681-31,393.

Dong, X., P. Minnis, T. P. Ackerman, E. E. Clothiaux, G. G. Mace, C. N. Long, and J. C. Liljegren, 2000: A 25-month database of stratus cloud properties generated from ground-based measurements at the ARM SGP site. *J. Geophys. Res*. **105**, 4529-4538.

Dong, X., and G. G. Mace, 2003: Profiles of low-level stratus cloud microphysics deduced from ground-based measurements. *J. Atmos. and Oceanic Tech.*, **20**, 42-53.

Dong, X., P. Minnis, and B. Xi, 2005: A climatology of midlatitude continental clouds fromthe ARM SGP Central Facility: Part I: Low-level cloud macrophysical, microphysical andradiative properties. *J. Climate*, **18**, 1391-1410.

Dolinar, E., X. Dong, B. Xi, A. Kennedy, J. Jiang, P. Minnis, and H. Su, 2013: Evaluation of CMIP GCMs simulated cloud fraction and TOA radiation budgets using NASA satellite observations. In prep. for *JGR-atmosphere*.

Duynkerke, P. G., H. Zhang, and P. T. Jonker, 1995: Microphysical and turbulent structure of nocturnal stratocumulus as observed during ASTEX. *J. Atmos. Sci.*, **52,** 2763–2777.

Garrett, T. J. and P. V. Hobbs, 1995: Long-range transport of continental aerosols over the Atlantic ocean and their effects on cloud structures. *J. Atmos. Sci*., **52**, 2977-2984.

Hartmann, D. L. and D. Short, 1980: On the use of earth radiation budget statistics for studies of clouds and climate. *J. Atmos. Sci.*, **37**, 1233–1250.

Houghton, J. T. and coauthors, 2001: Climate Change 2001: The Scientific Basic. Cambridge University Press.

Hudson, J. G. and H. Li, 1995: Microphysical contrasts in Atlantic Stratus. *J. Atmos. Sci*., **52**, 3031-3040.

Jefferson, A., 2010: Empirical estimates of CCN from aerosol optical properties at four remote sites, Atmos. *Chem. Phys.*, **10**, 6855-6861, doi:10.5194/acp-10-6855-2010.

Jiang, J. et al. 2012: Evaluation of cloud and water vapor simulations in CMIP5 climate models using NASA "A-train" satellite observations. *J. Geophys. Res.*, **117**, D14105, doi:10.1029/2011JD017237.

IPCC 2007: Climate change 2007: The physical science basis, Contribution of working group I to the fourth assessment report of IPCC. Cambridge Univ. Press.

Klein, S.A., and D.L. Hartmann, 1993: The seasonal cycle of stratiform clouds. *J. Clim.*, **6**, 1587-1606.

Klein, S. A., Y. Zhang, M. D. Zelinka, R. Pincus, J. Boyle, and P. J. Gleckler, 2013: Are climate model simulations of clouds improving? An evaluation using the ISCCP simulator. *J. Geophys. Res.*, **118**(3), 1329-1342, doi:10.1002/jgrd.50141.

Lilly, D. K, 1968: Models of cloud-topped mixed layers under a strong inversion. *Quart. J. Roy. Meteor. Soc.*, **94**, 292-309.

Liljegren, J. C., E. E. Clothiaux, G. G. Mace, S. Kato, and X. Dong, 2001: A new retrieval for cloud liquid water path using a ground-based microwave radiometer and measurements of cloud temperature. *J. Geophys. Res.*, **106**, 14 485-14 500.

Lin, W., M. Zhang, N. G. Loeb, 2009: Seasonal Variation of the Physical Properties of Marine Boundary Layer Clouds off the California Coast. *J. Climate*, **22**, 2624–2638.

Long, C. N., and Y. Shi (2008), An automated quality assessment and control algorithm for surface radiation measurements, *J. of the Open Atmos. Sci.*, **2**, 23-37.

Martin, G. M., D. W. Johnson, and A. Spice, 1994: The measurement and parameterization of effective radius of drops in warm stratocumulus clouds. *J. Atmos. Sci.*, **51,** 1823–1842.

Martin, G.M., D. P. Rogers, P. R. Jonas, P. Minnis, and D. A. Hegg, 1995: Observations of the interaction between cumulus clouds and warm stratocumulus clouds in the marine boundary layer during ASTEX. *J. Atmos. Sci.*, **52,** 2902–2922.

Mead, J. B., and K. B. Widener, 2005: W-band ARM cloud radar. Preprints, *32nd Int. Conf. on Radar Meteorology*, Albuquerque, NM, Amer. Meteor. Soc., P1R.3. [Available online at http://ams.confex.com/ams/pdfpapers/95978.pdf.]

Miles, N.L., J. Verlinde, and E.E. Clothiaux, 2000: Cloud-Droplet Size Distributions in low-level Stratiform Clouds. *J. Atmos. Sci.*, **57**, 295-311.

O'Dell C. W., F. J. Wentz, and R. Bennartz, 2008: Cloud liquid water path from satellite-based passive microwave observations: a new climatology over the global oceans. *J. Climate.* **21**: 1721–1739.

Paluch, J. R. and D. H. Lenschow, 1991: Stratiform cloud formation in the marine boundary layer. *J. Atmos. Sci.*, **48**, 2141-2158.

Platnick, S. and F. P. J. Valero, 1995: A validation of a satellite cloud retrieval during ASTEX. *J. Atmos. Sci.*, **52**, 2985-3001.

Rémillard, J., P. Kollas, E. Luke, and R. Wood, 2012: Marine boundary layer clouds observations in the Azores. *J Clim.*, **25**, 7381-7398.

Rossow, W.B., and R.A. Schiffer, 1991: International Satellite Cloud Climatology Project (ISCCP) cloud data products. *Bull. Amer. Meteor. Soc.* **72**, 2-20.

Soden, B. J., and G. A. Vecchi, 2011: The vertical distribution of cloud feedback in coupled ocean-atmosphere models. *Geophys. Res. Lett.*, **38**, L12704, doi:10.1029/2011GL047632

Slingo, A., 1990: Sensitivity of the earth's radiation budget to changes in low clouds. *Nature*, **343**, 49-51.

Stanfield, R., X. Dong, B. Xi, A. Gel Genio, P. Minnis, and J. Jiang: Assessment of NASA GISS CMIP5 and post-CMIP5 Model E simulated clouds and TOA radiation budgets using satellite observations: Part I: Cloud fraction and microphysical properties. In preparation for *J. Climate.*

Stephens, G. L., and C. M. R. Platt, 1987: Aircraft observations of the radiative and microphysical properties of stratocumulus and cumulus cloud fields. *J. Climate Appl. Meteor.*, **26,** 1243–1269.

Taylor, K. E., R. J. Stouffer, and G. A. Meehl, 2012: An overview of CMIP5 and the experiment design. *Bull. Amer. Meteor. Soc.*, **93**, 485–498.

Wielicki, B.A., R. D. Cess, M. D. King, D. A. Randall, and E. F. Harrison, 1995: Mission to planet Earth: Role of clouds and radiation in climate. *Bull. Am. Meteorol. Soc.*, **76**, 2125-2153.

Wood R., C. S. Bretherton, and D. L. Hartmann, 2002: Diurnal cycle of liquid water path over the subtropical and tropical oceans. *Geophys. Res. Lett.* **29**(23): 2092.

Wood, R., 2009: Clouds, Aerosol, and Precipitation in the Marine Boundary Layer (CAP-MBL). Available at http://www.arm.gov/publications/programdocs/doe-sc-arm-0902.pdf?id=94

Wood, R., 2012: Review: stratocumulus clouds. *Mon. Wea. Rev.*, **140**, 2373-2423.

Xi, B. and X. Dong, P. Minnis, and M. M. Khaiyer, 2010: A 10-year climatology of cloud cover and Vertical distribution derived from both surface and GOES observations over the DOE ARM SGP Site. *J. Geophys. Res.*,**115**, D12124, doi:10.1029/2009JD012800.

Xi, B., X. Dong, P. Minnis, and S. Sun-Mack, 2013: Validation of satellite-retrieved MBL cloud properties using DOE AMF measurements at the Azores. In preparation for JGR.

Yoo, H., and Z. Li, 2012: Evaluation of cloud properties in the NOAA/NCEP Global Forecaster System using multiple satellite product. *Climate Dyn.*, 10.1007/s00382-012-1430-0

Yoo, H., Z. Li, Y.-T. Hou, S. Lord, F. Weng, and H. W. Barker, 2013: Diagnosis and testing of low-level cloud parameterizations for the NCEP/GFS using satellite and ground-based measurements**.** *Climate Dynamics*, DOI 10.1007/s00382-013-1884-8.

Figures

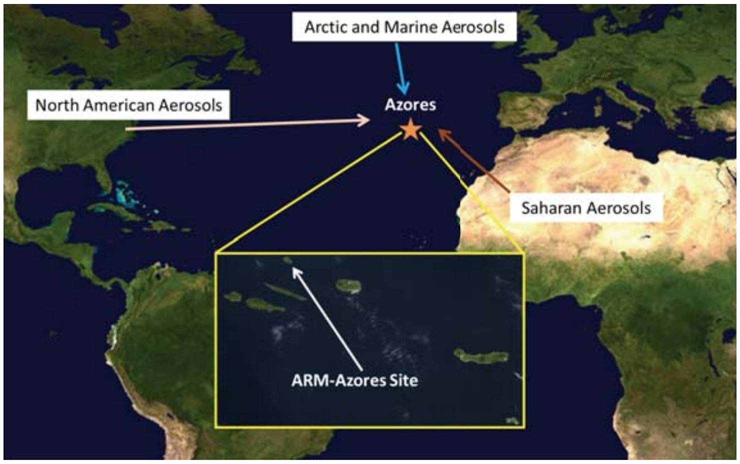

FIG 1. ARM AMF was deployed at the northern coast of the Graciosa Island (39.09°N, 28.03°W) in the Azores. The Azores was dominated by clean air masses but with periodic episodes of continentally polluted air masses from North America, Europe, and Saharan desert. (Figure 1 is modified based on NASA World Wind software at http://worldwind.arc.nasa.gov/index.html)

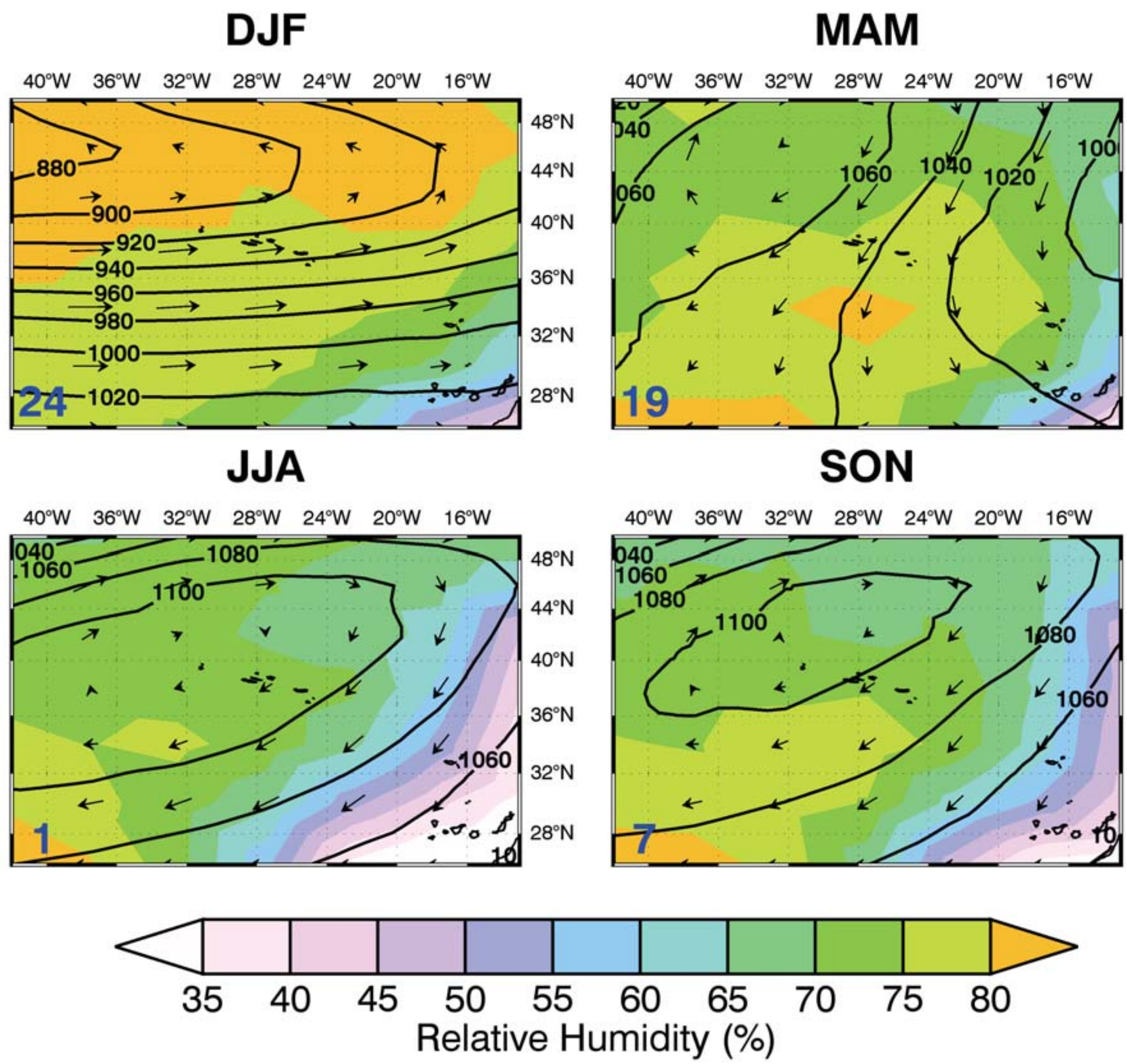

FIG. 2. 900 hPa Analaysis based on the NASA MERRA reanalysis during the period June 2009-December 2010. The grid box covers a range of latitudes from 26-50^{o}N and longitudes from 42-12^{o}W centered on the ARM Azores site. Shown are 900 hPa geopotential heights, wind vectors, and shaded contours of relative humidity. Four seasons are winter (DJF), Spring (MAM), summer (JJA) and Fall (SON).

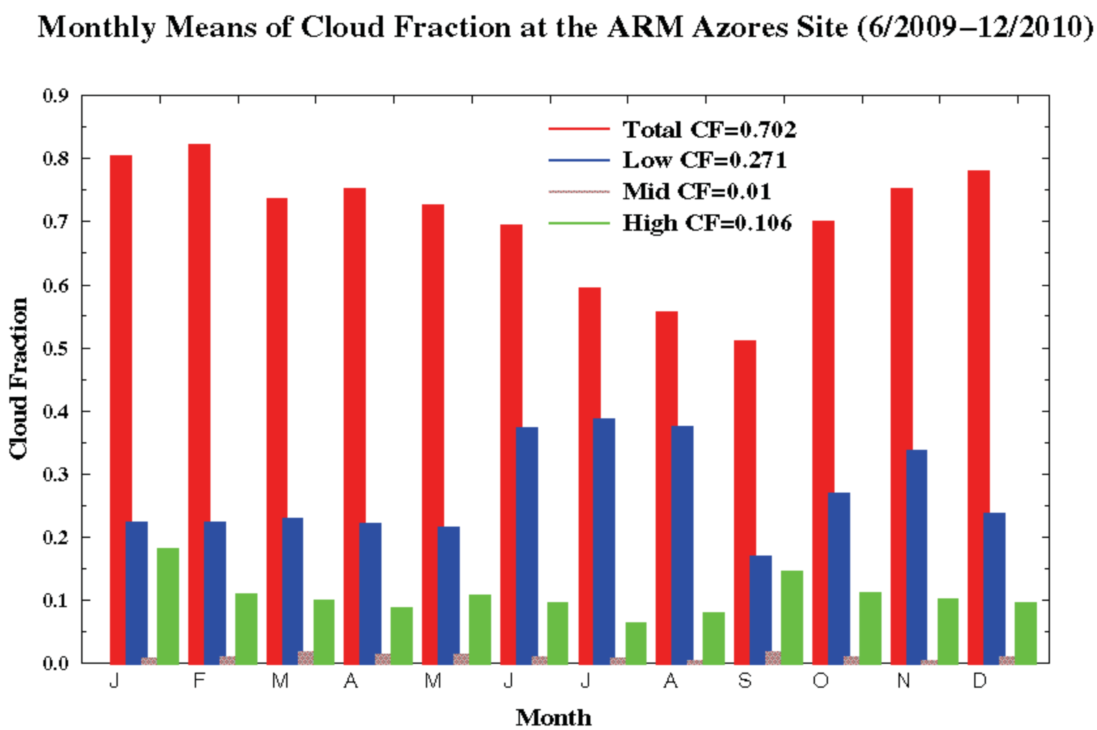

FIG. 3. Monthly mean cloud fractions derived from DOE ARM radar-lidar measurements during the DOE ARM Mobile Facility (AMF) June 2009-December 2010 deployment at Graciosa Island, Azores (39.09°N, 28.03°W). Total CF includes any clouds above the radar-lidar instruments. Single-layered clouds: Low CF ($Z_t \leq 3$ km), Mid CF ($Z_b > 3$ km, $Z_t \leq 6$ km), and High CF ($Z_t > 6$ km).

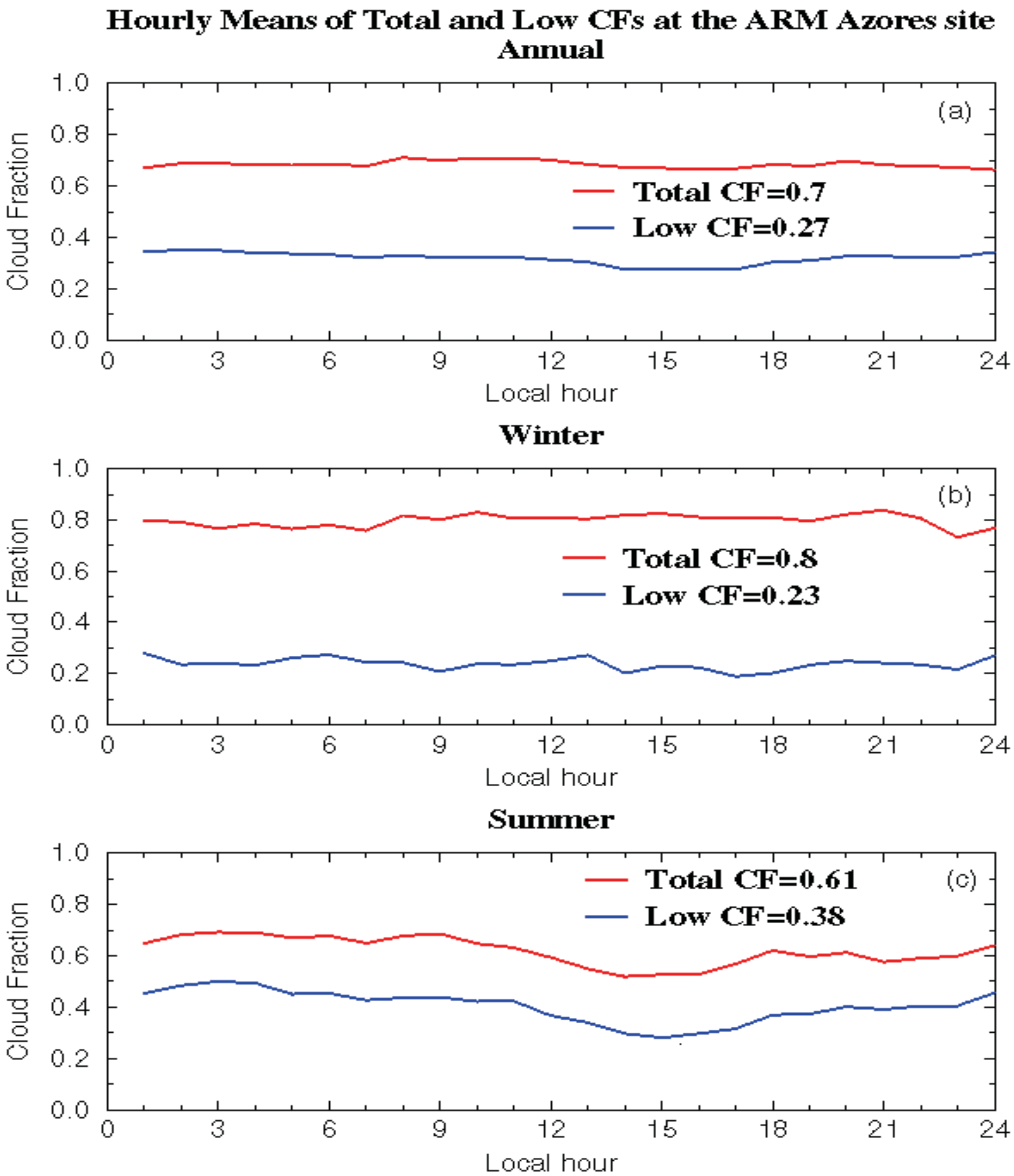

FIG. 4. Same as FIG. 3, except for hourly mean cloud fraction derived from ARM radar-lidar observations at the ARM Azores site during the 19-month period. Local hour at the ARM Azores site is UTC-1 hr.

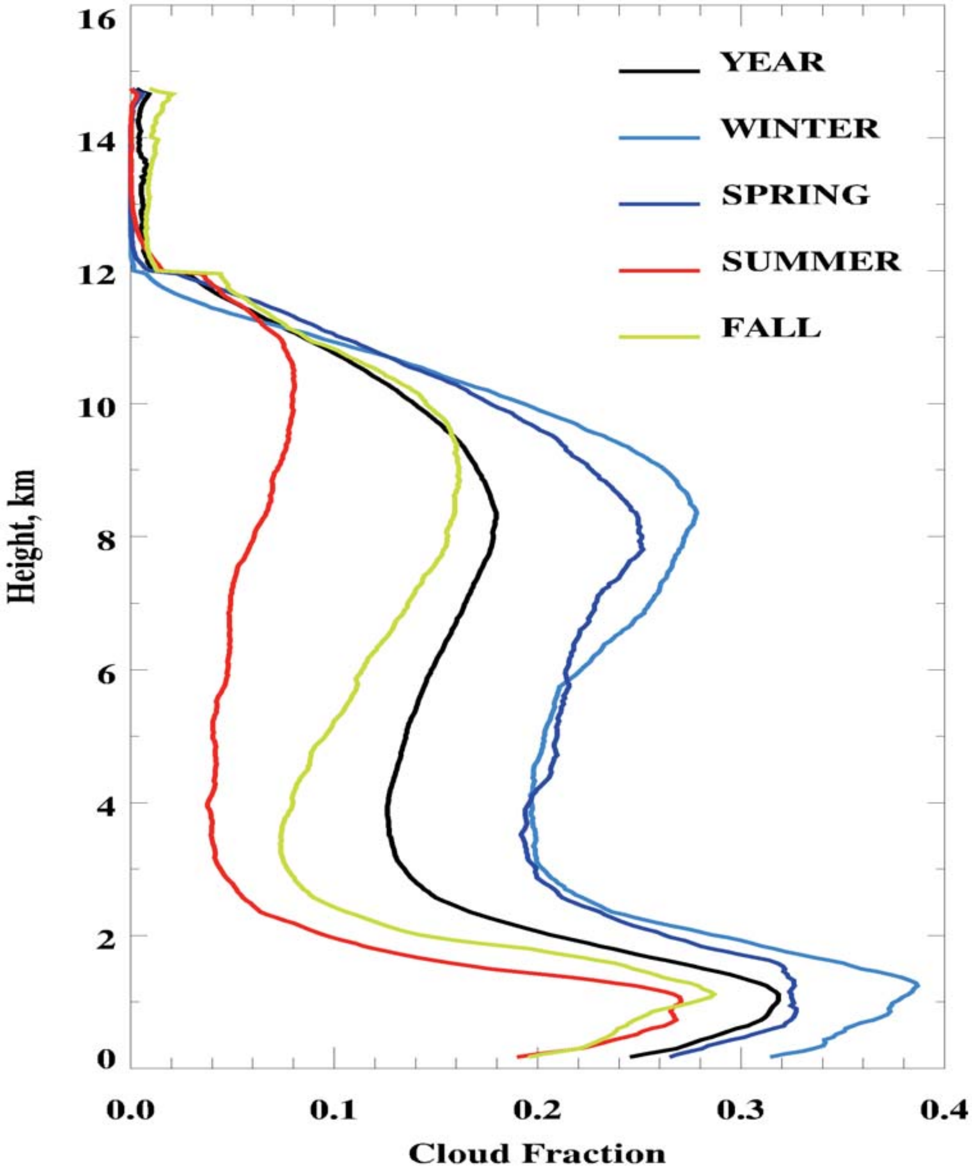

FIG. 5. Mean vertical distributions of CF derived from the ARM radar-lidar observations with a vertical resolution of 43 m and a temporal resolution of 5 min at the ARM Azores site, 06/2009-12/2010.

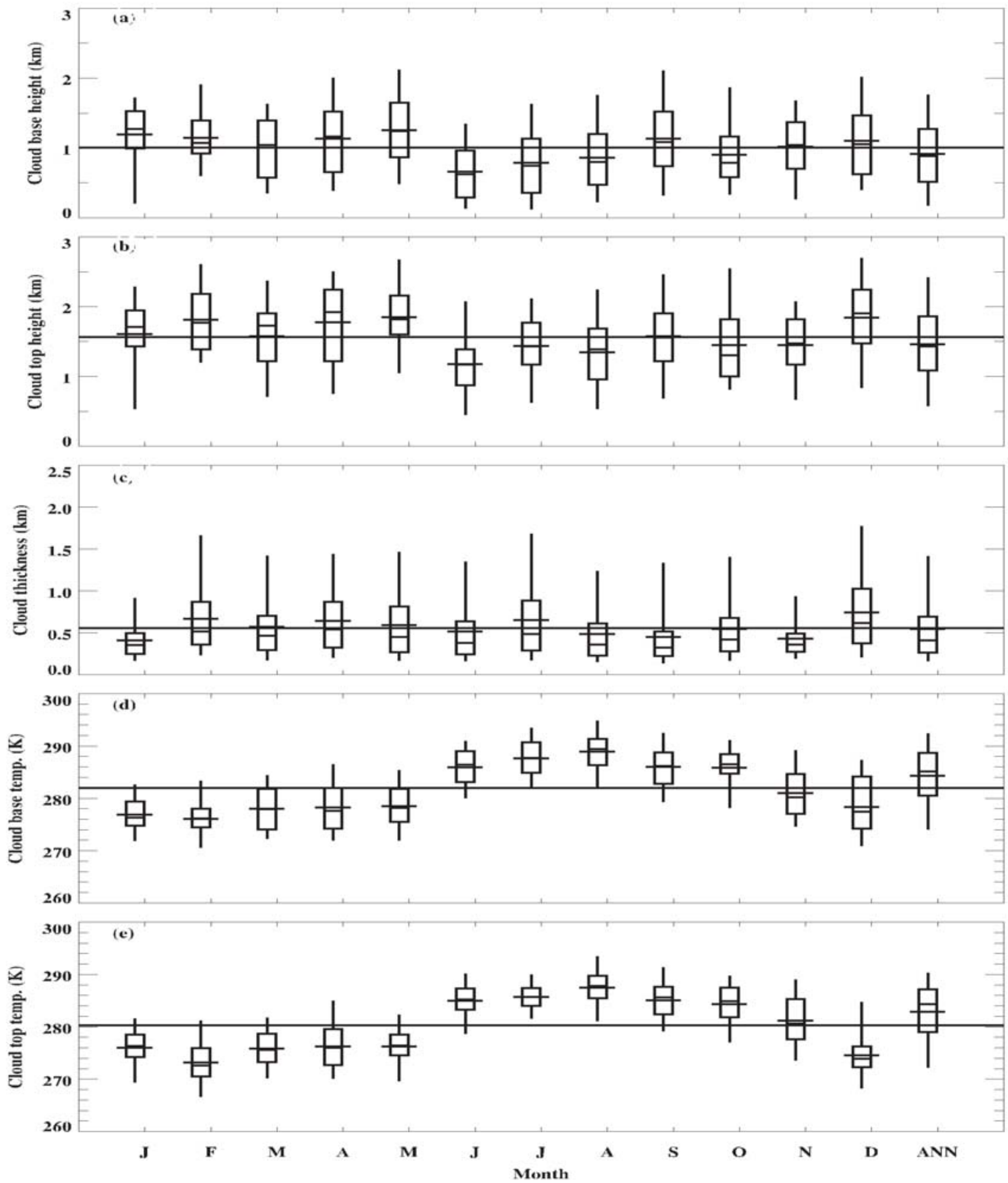

FIG. 6. Monthly mean daytime single-layered marine boundary layer (MBL) cloud macrophysical properties derived from a total of 19 months ARM Azores observations. Bottom and top of each whisker represent the 5th and 95th percentiles, bottom and top of each box represent 25th and 75th percentiles, and the shorter and longer lines across each box represent the median and mean, respectively. The distribution at the far right (ANN) of each plot shows cumulative statistics derived from all daytime data sets during the 19-month period, and the yearly average from entire dataset is drawn across the entire plot.

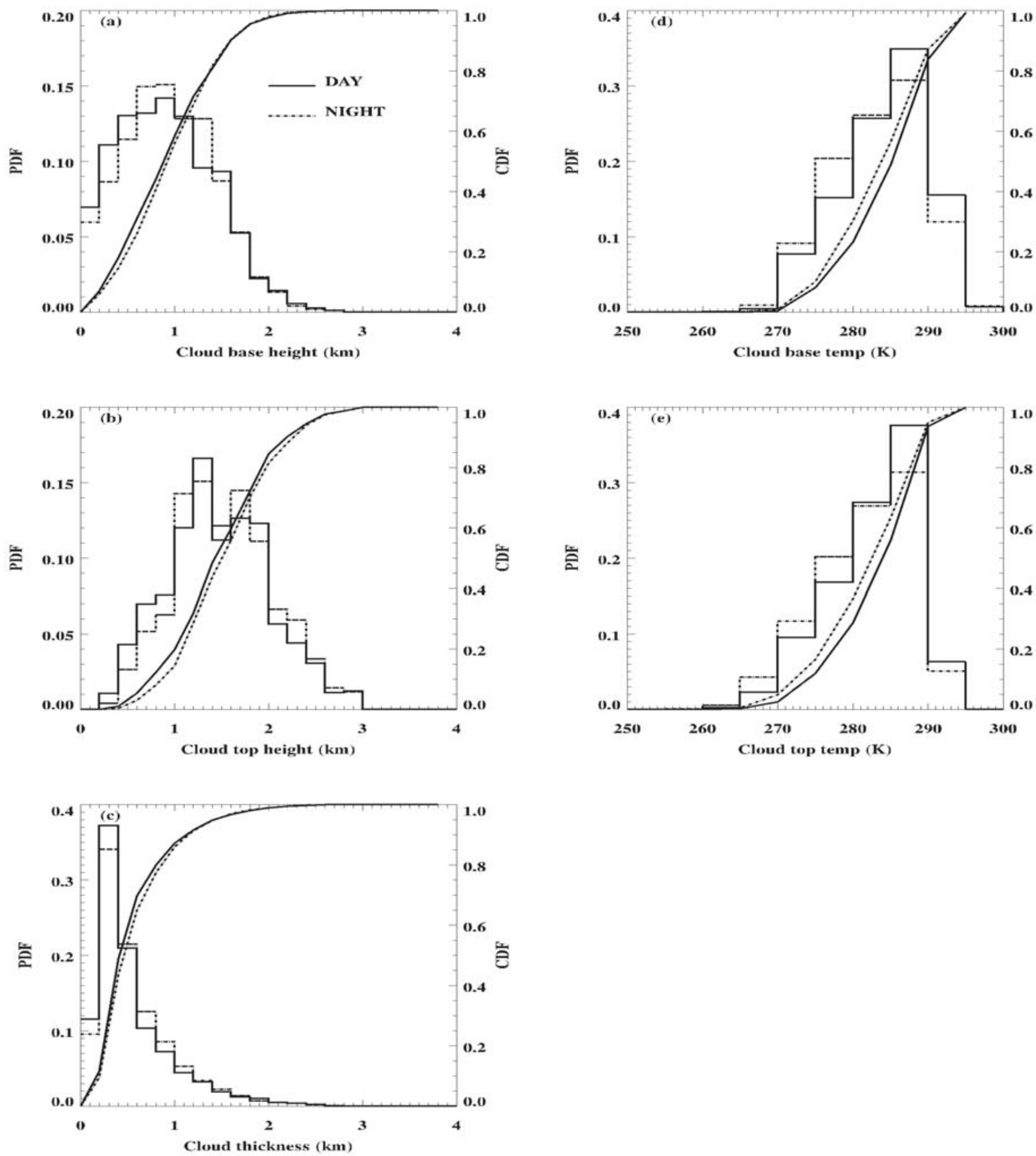

FIG. 7. Probability Distribution Functions (PDF) and Cumulative Distribution Functions (CDF) of single-layered MBL cloud macrophysical properties for both day (solid line) and nighttime (dashed line) from all 5-min samples at the ARM Azores site during the 19-month period.

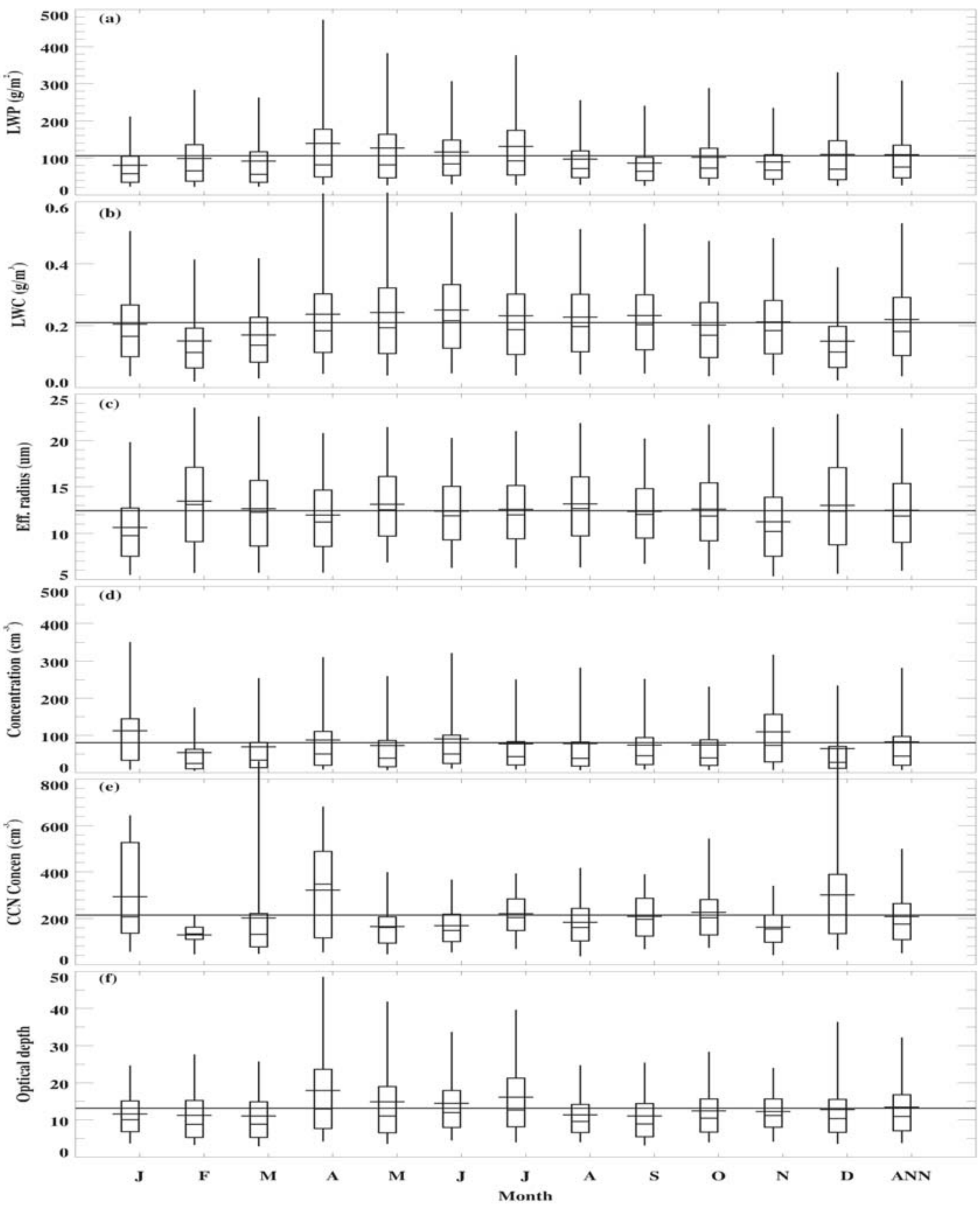

743

744 FIG. 8. Same as FIG. 6, except for daytime MBL cloud microphysical properties: (a) LWP, (b)
745 LWC, (c) cloud-droplet effective radius r_e and (d) number concentration N_d, and (f) optical depth,
746 as well as (e) surface CCN.
747

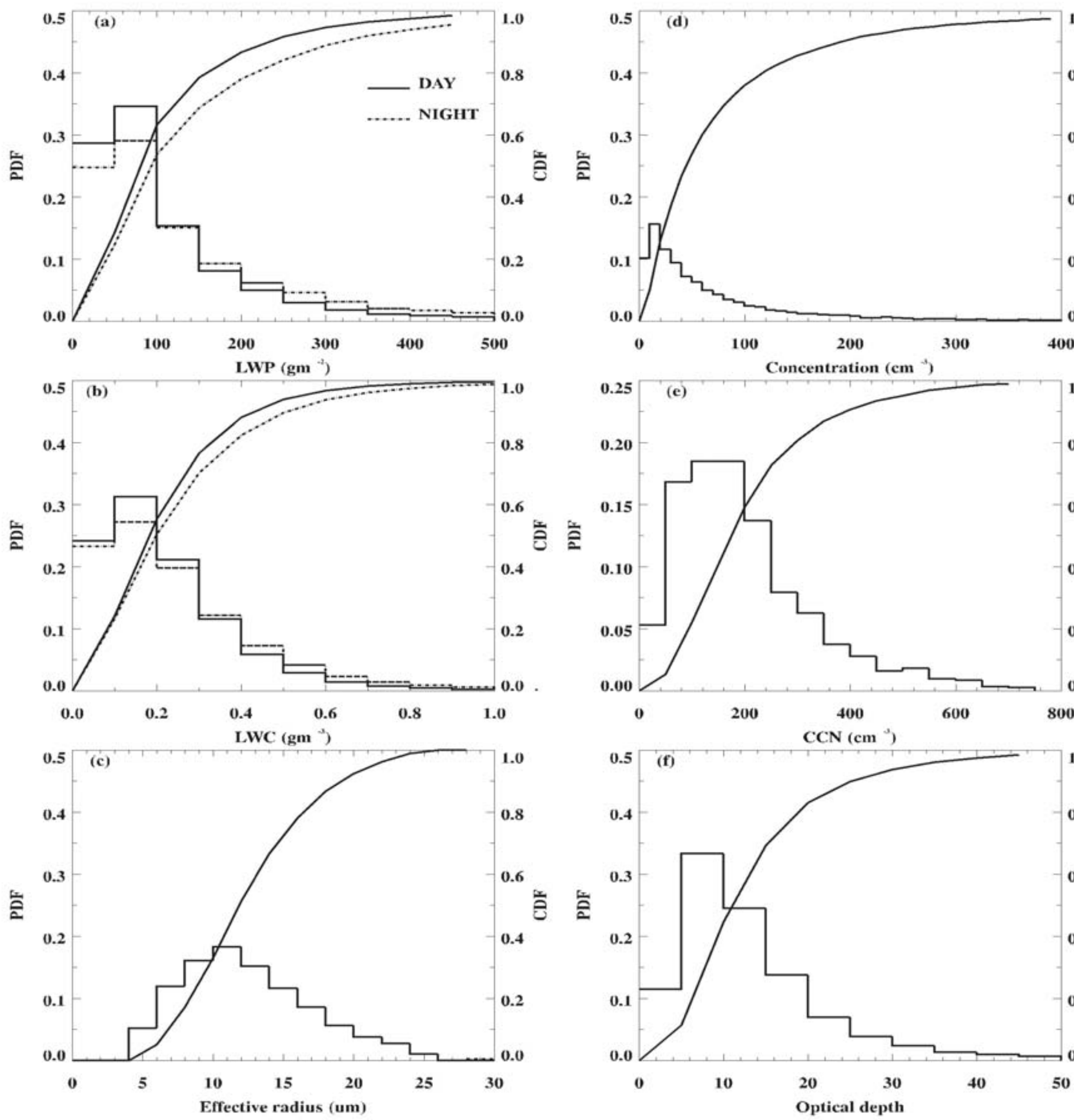

FIG. 9. Same as FIG. 7, except for MBL cloud microphysical properties and surface CCN.

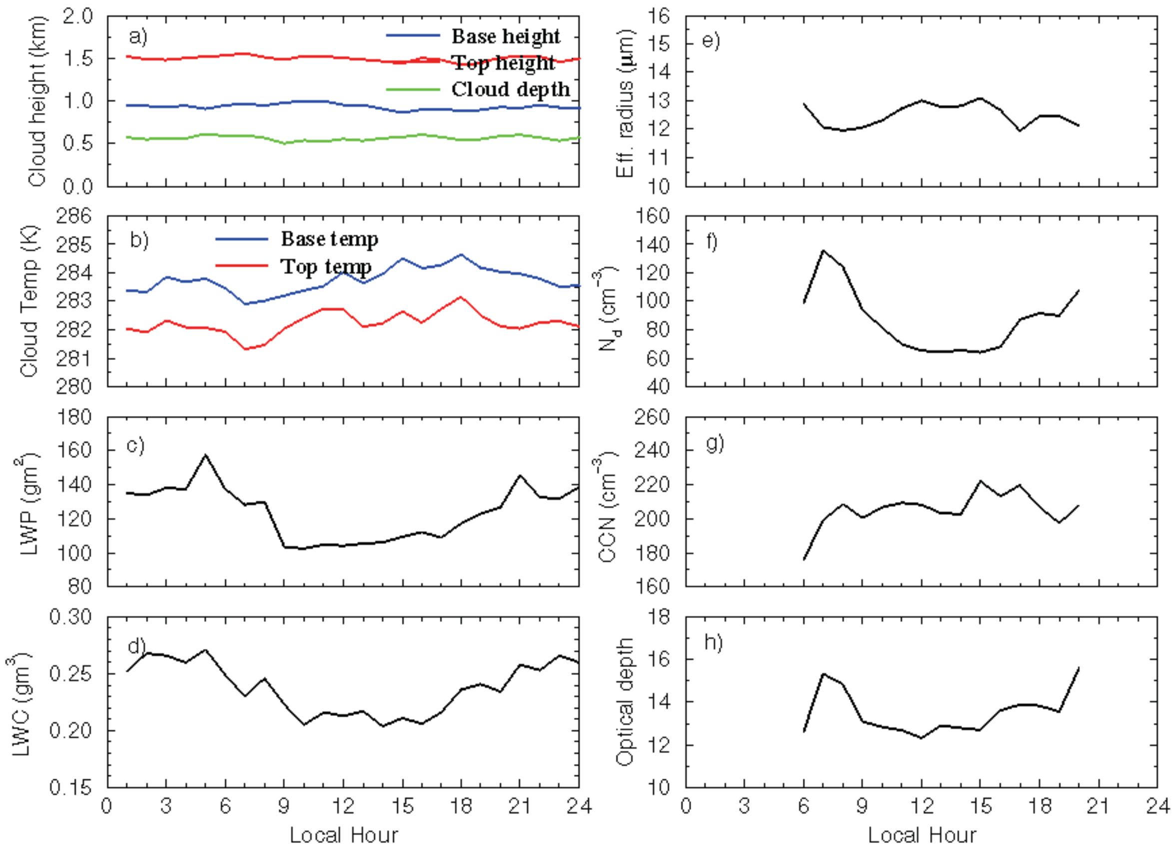

FIG. 10. Same as FIG. 4, except for hourly means of single-layered MBL clouds properties from both daytime and nighttime datasets. Only daytime r_e, N_d and optical depth, and surface *CCN* are plotted due to available retrievals.

TABLE 1. Cloud property measurement and retrieval methods used at the ARM AMF (Azores)

Cloud Parameter	Instruments/ Methods	Uncertainty	References
Cloud base height	Ceilometer	15 m	Rémillard et al. (2012)
Cloud base height	Micropulse lidar	30 m	Clothiaux et al. (2000)
Cloud top height	Microwave cloud radar	43 m	Rémillard et al. (2012)
Cloud base and top temperatures	Merged sounding	0.2 ^{o}C	ARM website www.arm.gov
Cloud LWP	Microwave radiometer	~20 gm^{-2} for LWP<200 ~10% for LWP >200	Dong et al. (2000); Liljegren et al. 2001
Cloud LWC	LWP/cloud thickness		
r_e	Parameterization r_e=2.07+2.49lwp+10.25γ-0.25μ_0 +20.28lwp*γ-3.14lwp*μ_0	~ 10% for daytime	Dong et al. (1997, 1998, 2002)
N_d	Parameterization $N_d = lwc/[\frac{4}{3}\pi\rho_w r_e^3 \exp(-3\sigma_X^2)]$	~ 20-30% for daytime	Dong et al. (1997, 1998, 2002)
τ	Parameterization τ=1.5*lwp/r_e	~ 10 % for daytime	Dong et al. (1997, 1998, 2002)
CCN	AMF Aerosol Observing System	~	ARM Webpage: www.arm.gov (Jefferson, A., 2010)
γ	SW↓(cloud)/SW↓(clear)	~ 5% for daytime	Long and Shi (2008)

TABLE 2. Summary of 10 cloud categories at the ARM Azores site (06/2009-12/2010)

Cloud type	Definition (km)	Annual	Winter	Summer
1	Single low, < 3 km	0.271	0.228	0.377
2	Single middle, 3-6 km	0.01	0.009	0.007
3	Single high, > 6 km	0.106	0.128	0.078
4	Middle over low, contiguous	0.022	0.034	0.009
5	High over middle, contiguous	0.023	0.033	0.007
6	High over both mid and low, contiguous	0.036	0.064	0.007
7	Middle over low, non-contiguous	0.02	0.028	0.011
8	High over middle, non-contiguous	0.025	0.028	0.01
9	High over low, non-contiguous	0.103	0.156	0.032
10	High over mid and low, non-contiguous	0.085	0.089	0.074
Sum	**Total CF**	**0.70**	**0.80**	**0.613**

TABLE 3. Seasonal and yearly averages, standard deviations, medians, and modes of various cloud parameters derived from the 19-month ARM Azores dataset

	Winter		Spring		Summer		Autumn		Year	
	Day	Night	Day	Night	Day	Night	Day	Night	Day	Night
CF	0.231	0.215	0.215	0.212	0.352	0.370	0.259	0.284	0.282	0.295
Z_{base}, km	1.14 0.48 1.15 1.5	1.12 0.4 1.12 1.1	1.15 0.51 1.17 1.5	1.08 0.52 1.06 0.7	0.76 0.47 0.73 0.3	0.79 0.47 0.76 0.7	1.0 0.48 0.96 0.09	0.98 0.48 0.92 0.9	0.92 0.51 0.88 0.9	0.95 0.49 0.91 0.9
Z_{top}, Km	1.77 0.53 1.82 1.9	1.78 0.47 1.73 1.7	1.75 0.54 1.82 1.9	1.71 0.56 1.69 1.75	1.31 0.50 1.3 1.3	1.35 0.48 1.3 1.3	1.47 0.51 1.43 1.9	1.51 0.51 1.52 1.1	1.46 0.54 1.43 1.3	1.52 0.52 1.52 1.3
ΔZ, Km	0.63 0.45 0.49 0.4	0.66 0.4 0.55 0.3	0.6 0.42 0.48 0.3	0.63 0.46 0.49 0.3	0.55 0.43 0.4 0.3	0.56 0.42 0.42 0.3	0.48 0.34 0.37 0.3	0.53 0.36 0.42 0.3	0.55 0.41 0.41 0.3	0.58 0.41 0.45 0.3
T_{base}, K	277.2 4.5 276.4 277.5	276.7 3.8 276.6 277.5	278.3 4.4 277.9 277.5	278.5 4.8 278.5 277.5	287.4 3.9 287.7 287.5	287.3 4.0 287.5 287.5	283.8 4.9 285.0 287.5	283.2 5.2 283.8 287.5	284.3 5.7 285.1 287.5	283.2 6.0 283.8 287.5
T_{top}, K	274.7 4.5 274.6 272.5	274.2 4.7 274.5 277.5	276.2 3.9 276.1 277.5	276.1 4.4 276.4 277.5	286.0 3.5 286.0 287.5	285.8 3.6 286.3 287.5	283.1 4.8 284.1 287.5	282.2 5.2 283.1 287.5	282.9 5.8 284.3 287.5	281.7 6.2 282.8 287.5
lwp, gm^{-2}	99.0 92.0 65.7 25	147.4 144.9 90.6 25	121.8 119.9 75.2 25	138.4 133.4 87.5 75	114.4 96.3 81.4 75	148.8 129.6 100.9 75	93.3 76.9 68.7 75	124.6 115.4 84.5 75	108.7 96.0 75.4 75	139.6 129.1 91.6 75
lwc, gm^{-3}	0.16 0.14 0.12 0.05	0.23 0.21 0.17 0.05	0.22 0.18 0.17 0.15	0.24 0.18 0.19 0.16	0.24 0.17 0.2 0.15	0.29 0.26 0.23 0.16	0.21 0.15 0.18 0.15	0.25 0.19 0.2 0.16	0.22 0.17 0.18 0.15	0.26 0.22 0.2 0.16
r_e, μm	12.4 5.1 11.5 9		12.6 4.6 12.0 11		12.7 4.4 12.2 11		12.0 4.6 11.2 11		12.5 4.6 11.9 11	
N, cm^{-3}	75.4 117.7 36.3 5		76.8 113.4 40.3 15		82.5 137.9 43.5 15		89.1 110.8 52.4 15		82.6 126.2 44.1 15	
CCN, cm^{-3}	265.6 222,7 173.9 125		235.3 195.9 162.7 75		192.5 109.8 173.8 125		196.1 114.8 180.4 175		207.3 143.8 175.0 125	
τ	12.1 8.4 10.0 7.5		14.9 12.7 10.9 7.5		14.0 9.7 11.4 7.5		12.1 7.3 10.5 7.5		13.5 9.6 11.0 7.5	

TABLE 4. MBL cloud *LWC*, r_e, N_d and *CCN* retrieved from ARM AMF-Azores measurements in this study and measured by aircraft during ASTEX (June 1992)

Location	Air mass	*LWC* gm^{-3}	r_e μm	N_d cm^{-3}	*CCN* cm^{-3}	Source
Azores Annual mean, daytime	Maritime with periodic pollution	0.219	12.5	82.6	207.3	This study
Azores June, daytime	Maritime with periodic pollution	0.25	12.4	90.6	168.5	This study
Azores, ASTEX	Maritime	0.164	8.2	86	163	Yum and Hudson (2002)
Azores, ASTEX	Continental	0.119	6.1	183	1023	Yum and Hudson (2002)
Different IOPs	Maritime	0.18	9.6	74		Miles et al. (2000)
Azores, ASTEX	Maritime	0.15-0.35	9.5-13.4	47		Albrecht et al. (1995)
Azores, ASTEX	Nocturnal stratus	0.01-0.37	5.8-9.8	100		Duynkerke et al. (1995)
Azores, ASTEX	Sc	0.15	10.8	50		Martin et al. (1994 and 1995)
Azores, ASTEX	Maritime		9.4-13.9			Platnick and Valero (1995)
Azores, ASTEX June 12	Maritime	0.23	7.3	174	30-100	Garrett and Hobbs (1995)
Azores, ASTEX June 22	Continental	0.21	5.3	457	100-800	Garrett and Hobbs (1995)
Azores, ASTEX June 17	Continental	0.2	5.4	220	668	Hudson and Li (1995)
Azores, ASTEX June 17	Maritime	0.2	12.2	35	116	Hudson and Li (1995)
Off east coast of Australia	Maritime	0.16	11.6			Stephens and Platt (1987)